Thermophoresis at a charged surface: the role of hydrodynamic slip

Julien Morthomas, Alois Würger

Thermophoresis at a charged surface: the role of hydrodynamic slip

Julien Morthomas and Alois Würger
CPMOH, Université Bordeaux 1 & CNRS, 351 cours de la Libération, 33405 Talence, France

By matching boundary layer hydrodynamics with slippage to the force-free flow at larger distances, we obtain the thermophoretic mobility of charged particles as a function of the Navier slip length b. A moderate value of b augments Ruckenstein's result by a term $2b/\lambda$ where λ is the Debye length. If b exceeds the particle size a, the enhancement coefficient a/λ is independent of b but proportional to the particle size. Similar effects occur for transport driven by a salinity gradient or by an electric field.

PACS numbers: 82.45.-h, 82.70.-y, 47.61.Fg

I. INTRODUCTION.

In recent years the thermally driven motion of charged colloids has attracted much attention, and a variety of surprising phenomena have been observed [1, 2]. The Soret effect of a micellar solution was shown to vary with the surfactant concentration [3], and unexpected dependencies on temperature and electrolyte composition were reported for suspensions of nanoparticles and macromolecular solutions [4–13]. A thermal gradient has been used as a trap for DNA in a microchannel with ambiant flow [14].

Transport of charged colloids arises from a generalized external force acting on the electric double layer at a particle-fluid interface. The thermophoretic mobility is defined through the drift velocity of the solute induced by a temperature gradient in the solvent fluid,

$$\mathbf{u} = -D_T \boldsymbol{\nabla} T. \tag{1}$$

There are two different routes to calculating the transport coefficient D_T; the first one relies on low-Reynolds number hydrodynamics and the thermal force density on the fluid in the boundary layer [15–21], whereas the second one expresses the velocity $\mathbf{u}$ through the particle mobility and a force that is given by the gradient of the double-layer energy [22–24].

Most parameters of a charged colloid depend on temperature, such as the solute surface potential and the solvent permittivity, viscosity, and salinity. Thus in most cases, it is not obvious to single out the physical mechanism underlying the observed dependencies. For example, the transport coefficient D_T changes sign as a function of temperature and electrolyte composition; increasing temperatures and high pH values favor an inverse Soret effect $D_T < 0$. It was realized only recently that the thermoelectric field of the electrolyte solution plays a major role in thermophoresis and often determines the sign and magnitude of D_T [6, 20].

The size dependence of D_T has been much debated in the last years. Experiments on polystyrene beads in aqueous solution reported a linear variation $D_T \propto a$ with the particle radius over almost two orders of magnitude [7]; on the other hand, a constant D_T was found for droplets in microemulsions, and polystyrene beads [9, 11, 12].

From low-Reynolds number hydrodynamics with no-slip boundary condition at the particle-fluid interface, it is well known that any transport coefficient is constant with respect to the particle size, as long as the latter is larger than the Debye length λ [25]. At moderate electrolyte strength, λ takes typical values of a few nanometers, thus satisfying $\lambda \ll a$. Accordingly, Ruckenstein obtained a constant D_T [15]; this result was confirmed by several authors [16–20]. As a possible explanation for the experimental findings of Ref. [7], we noted in a previous paper that hydrodynamic slippage at the particle surface would give rise to linear dependence of D_T on the particle size [21].

In the present work, we derive the thermophoretic mobility as a function of the particle size a, the Debye length λ, and the slip length b. We discuss the dependence on these different length scales and, in particular, recover the above mentioned limiting cases of constant D_T and $D_T \propto a$. In Sect. 2 we obtain the general expression for the velocity change through the boundary layer. In Sect. 3 we show how a finite slip length modifies thermophoresis due to temperature and permittivity gradients; Sect. 4 discusses similar effects in a non-uniform electrolyte. We conclude with a discussion of the main results.

II. BOUNDARY LAYER HYDRODYNAMICS.

The boundary conditions at a solid-fluid interface have been debated since the early days of fluid mechanics; Navier proposed that a sheared fluid could slip along the surface, with the velocity jump being proportional to the applied shear rate. At a macroscopic scale, the fluid sticks to the solid surface, suggesting continuity of the velocity field. On the scale of microns or even nanometers, however, various measurements provide evidence for the occurrence of hydrodynamic slippage [26, 27]. On a molecular level, slip has been explained in terms of the weak adherence of the solvent to the solid surface. Simulations of the molecular dynamics at a charged interface related the slip length to van der Waals force parameters of the non-wetting fluid and to ion-specific interactions [28]. These simulations show that continuum hydrodynamics provide a good description of the fluid motion

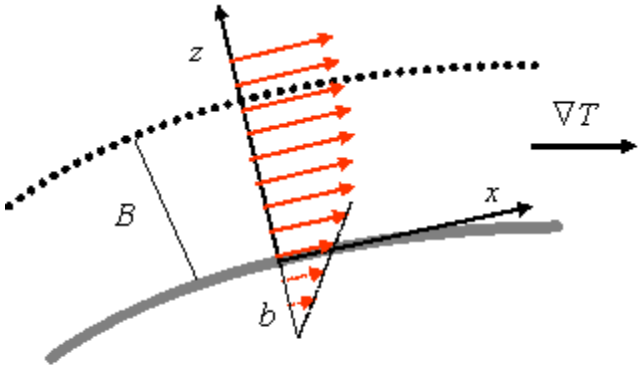

FIG. 1: Schematic view of the fluid velocity field in the boundary layer close to a particle of radius a. The external field acting on the electric double layer accelerates the charged fluid with respect to the solid. A finite surface velocity v_0 arises from hydrodynamic slip in a molecular layer (thick grey line); the slip length b is defined as the distance where the linear velocity profile would vanish. At a distance B, well beyond the electric double layer, the fluid attains the boundary velocity v_B.

even on the scale of nanometers, and that slip occurring in a few molecular layers may significantly accelerate externally driven transport, such as the flow in a microchannel.

In a continuum picture, the shear stress Σ_0 and the resulting slip velocity v_0 are related through Navier's boundary condition

$$\eta v_0 = b\Sigma_0, \tag{2}$$

where η is the fluid viscosity and b a material specific constant that has the dimension of a length. The latter parameter accounts for the reduced mocular viscosity at the interface. Various experiments confirm the linear stress-velocity relation, but others indicate a non-linear behavior, i.e., a slip length b that depends on the shear rate [26, 27].

A particle of radius a exerts on the surrounding fluid the effective force density f_x, including the excess hydrostatic pressure [19, 20], which is finite only close to the surface and vanishes at distances of the order B. The normal component of the fluid velocity within the boundary layer is zero, and its parallel component satisfies Stokes' equation, $\eta\partial_z^2 v_x + f_x = 0$, with constant hydrostatic pressure. It turns out convenient to consider the fluid motion in the frame attached to the particle. The integral of $\eta\partial_z^2 v_x + f_x = 0$ gives the shear stress $\Sigma_{xz} = \eta\partial_z v_x$. Its values at the surface Σ_0 and at the outer side of the boundary layer are related by

$$\Sigma_B = \Sigma_0 - \int_0^B dz f_x \equiv \Sigma_0 - \Delta\Sigma. \tag{3}$$

Integrating once more gives the parallel component of the fluid velocity $v_x(z)$. With the finite value at the particle surface $v_0 = v_x(0)$ we have well beyond the charged layer

$$v_B = v_0 + \frac{1}{\eta}\int_0^B dz z f_x \equiv v_0 + \Delta v. \tag{4}$$

The boundary velocity v_B is the sum of two contributions of different physical origin. The intrinsic slip velocity v_0 arises if the fluid molecules do not fully adhere to the solid. The velocity change through the boundary layer Δv, sometimes referred to as apparent slip [25], is due to the forces exerted by the surface on the fluid in the boundary layer.

The above Eqs. (2-4) are closed by matching Σ_B and v_B to the fluid flow beyond the boundary layer. In this range, the velocity field is solution of the force-free Stokes equation $\eta\boldsymbol{\nabla}^2\mathbf{v} = 0$ in three dimensions [30, 31]. For a uniform particle surface, the boundary velocity depends on the polar angle as

$$v_B = \bar{v}_B \sin\theta.$$

The normal and tangential components of the fluid flow beyond the boundary layer ($r \geq \tilde{a} \equiv a + B$) vary as $v_r \propto [1 - (\tilde{a}/r)^3]$ and

$$v_t = v_B\left(\frac{2}{3} + \frac{1}{3}\frac{\tilde{a}^3}{r^3}\right).$$

Since the normal velocity v_r vanishes at $r = \tilde{a}$, the off-diagonal stress in spherical coordinates reads [31]

$$\Sigma_{rt} = \eta\left(\frac{dv_t}{dr} - \frac{v_t}{r}\right).$$

With $\tilde{a} \simeq a$, we find the stress at the outer side of the boundary layer

$$\Sigma_B = -\frac{2\eta v_B}{a}. \tag{5}$$

For an inhomogeneous particle surface [32], the tangential velocity takes a more general form $v_t = \sum_n c_n(\theta) r^{-n}$ and modifies the numerical prefactor in Σ_B accordingly.

We briefly discuss the role of curvature in the matching condition (5). The change $\Delta\Sigma$ through the boundary layer has been calculated with $\Sigma_{xz} = \eta\partial_z v_x$, i.e., the shear stress has been taken as the normal derivative of the tangential velocity. On the other hand, Eq. (5) has been obtained from the above expression Σ_{rt} in spherical coordinates that comprises, besides the normal derivative $\partial_r v_t$, the term $-v_t/r$ accounting for the finite curvature of the interface. Indeed, outside the boundary layer, the normal derivative $\partial_r v_t$ of the force-free flow $\partial_r v_t$ and the

curvature term $-v_t/r$ are of the same order of magnitude; thus both have to be retained. As shown in Ref. [33] for Navier's slip condtion (2), the curvature contribution to the shear stress can be written alternatively in terms of the normal derivative $\Sigma_{xz} = \eta\partial_z v_x$ with an effective slip length $1/b_{\rm eff} = 1/b + 1/a$.

Eqs. (2-5) determine the boundary velocity v_B as a function of the slip length

$$v_B = \frac{\Delta v + b\Delta\Sigma/\eta}{1 + 2b/a}. \tag{6}$$

For Stokes boundary conditions with zero slip length one has $v_B = \Delta v$, whereas the opposite limit $b \to \infty$ leads to $v_B = \frac{1}{2}a\Delta\Sigma/\eta$. In some aspects hydrodynamic slippage at a solid-fluid interface is similar to the flow on a gas bubble in a viscous liquid [25, 34], which is described by Hadamard-Rybczynski boundary conditions. In view of (2) the limit of zero shear stress at the interface, $\Sigma_0 = 0$, corresponds to $b \to \infty$ [30].

So far we have considered the reference frame where the particle is immobile, that is why v_r and v_t are finite at $r \to \infty$. Transformation to the laboratory frame gives the velocity of the moving particle, $\mathbf{u} = -\langle \mathbf{e}_v v_B\rangle$; the orientational average along the particle surface $\langle ...\rangle$ results in [25]

$$u = -\frac{2}{3}\bar v_B. \tag{7}$$

Eqs. (6) and (7) apply to any force density exerted on the fluid in the boundary layer. In the remainder of this paper we discuss in detail the case of thermophoresis, and then treat a non-uniform electrolyte with a salinity gradient and a spontaneaous electric field.

III. THERMOPHORESIS.

We discuss transport driven by a temperature gradient in an otherwise uniform electrolyte [15]. In order not to encumber the equations, we resort to the Debye-Hückel approximation. The charged particle exerts on a unit volume of the surrounding fluid the force density [19, 20]

$$\mathbf{f} = \frac{\varepsilon\psi^2}{2\lambda^2}(1 + \alpha + \tau)\frac{\boldsymbol{\nabla} T}{T},$$

where $\psi = \psi_0 e^{-z/\lambda}$ is the electric potential in the boundary layer and ψ_0 the value at the surface. The logarithmic derivative $\tau = -d\ln\varepsilon/d\ln T$ accounts for the temperature dependence of the permittivity $\varepsilon(T)$; in water it varies from $\tau = 1.25$ at 0 °C to $\tau = 1.5$ at 50 °C. The parameter α describes the spatial variation of the salinity [18, 20],

$$\frac{\boldsymbol{\nabla} n_0}{n_0} = -\alpha_0\frac{\boldsymbol{\nabla} T}{T}.$$

The reduced Soret coefficient α of the electrolyte solution takes values $\alpha = 0.8$ for NaCl and $\alpha = 3.4$ for NaOH.

Integrating Eqs. (3) and (4) we find with $T_x = dT/dx$ the changes of velocity and shear stress,

$$\Delta v = \frac{\varepsilon\psi_0^2}{8\eta}(1 + \alpha + \tau)\frac{T_x}{T}, \qquad \Delta\Sigma = \frac{\varepsilon\psi_0^2}{4}(1 + \alpha + \tau)\frac{T_x}{T}.$$

Insertion in the general relation (6) gives the boundary velocity

$$v_B = \frac{\varepsilon\psi_0^2}{8\eta}(1 + \alpha + \tau)\frac{1 + 2b/\lambda}{1 + 2b/a}\frac{T_x}{T}.$$

Identifiying $u = -\frac{2}{3}\bar v_B$ and $u = -D_T T_x$ we obtain the thermophoretic mobility

$$D_T = \frac{\varepsilon\psi_0^2}{12\eta T}(1 + \alpha + \tau)\frac{1 + 2b/\lambda}{1 + 2b/a}, \tag{8}$$

which constitutes a main result of the present paper.

We discuss limiting cases with respect to the lengths a, b, λ. For zero slip $b = 0$ and using the surface potential $\psi_0 = \lambda\sigma/\varepsilon$, we have

$$D_T^{(0)} = \frac{\sigma^2\lambda^2}{12\eta\varepsilon T}(1 + \alpha + \tau)$$

and thus recover the variation with the square of the Debye length obtained in [15, 17, 19]. In the opposite case of large slip length $a \ll b$, Eq. (8) confirms the relation $D_T = (a/\lambda)D_T^{(0)}$ obtained previously in [2, 21]. In the intermediate case $\lambda \ll b \ll a$, we find a linear law $D_T \propto \lambda$, with an enhancement factor $D_T/D_T^{(0)} = 2b/\lambda$ that is twice that of the electrophoretic mobility $\mu/\mu_0 = b/\lambda$ [29]. The additional factor 2 arises since the thermal force is quadratic in the surface potential ψ_0, whereas electrophoresis is linear in ψ_0.

IV. THERMOELECTRICITY

Recently it has become clear that the Soret effect of charged colloids is to a large extent determined by the thermoelectric effect of the electrolyte solution [6, 20], that is, the macroscopic field induced by thermal diffusion of the mobile ions,

$$\mathbf{E}_\infty = \delta\alpha\frac{k_B\boldsymbol{\nabla} T}{e},$$

where e is the elementary charge and $\delta\alpha$ the reduced Seebeck coefficient. Typical values are $\delta\alpha = 0.6$ for NaCl and $\delta\alpha = -2.7$ for NaOH [20]. This electric field drives the colloidal particles to the cold or to the warm, depending on the sign of $\delta\alpha$ and of the surface charge σ. Note that this effect differs from that studied in [36], with an electric field $E_{\rm ind} \propto (D_+ - D_-)$ proportional to the difference of diffusion coeffiicients of co-ions and counterions.

The thermoelectric effect modifies the thermophoretic mobility according to [20],

$$D_T - \delta\alpha_b\frac{e\psi_0}{4\eta\pi\ell_B T} = D_T - \delta\alpha_b\frac{\sigma\lambda k_B}{e}, \tag{9}$$

where the reduced Seebeck coefficient $\delta\alpha_b$ accounts for a finite slip length. Eq. (8) shows how the first term depends on the slip length b. Here we derive the corresponding relation for $\delta\alpha_b$.

The external electric field $\mathbf{E}_\infty$ exerts on the charged fluid in the boundary layer the force

$$\mathbf{f} = \rho\mathbf{E}_\infty, \tag{10}$$

where $\rho = -2e\sinh(e\psi/k_BT)$ is the charge density in the electric double layer. The permittivity of water being much larger than that of most materials, the electric field hardly penetrates in the particle; close to the particle the vector $\mathbf{E}_S$ is parallel to the surface, and its magnitude $E_S = \frac{3}{2}E_\infty \sin\theta$ is enhanced by a factor $3\varepsilon/(2\varepsilon+\varepsilon_P) \approx \frac{3}{2}$ with respect to the value at infinity E_∞. For a homogeneous surface the integrals in (3) and (4) are readily related to the electrostatic properties of the charged surface. From direct integration or comparison with known results for electrophoresis [35], we obtain the stress and velocity changes through the boundary layer in terms of the surface charge density σ and the surface potential ψ_0,

$$\Delta\Sigma = -\sigma E_S, \quad \Delta v = -\frac{\varepsilon\psi_0}{\eta}E_S. \tag{11}$$

Note that the ratio of the velocity change Δv and E_S is identical to the Helmholtz-Smoluchowski mobility $\mu_0 = \varepsilon\psi_0/\eta$ [35]; this does not come as a surprise, since the thermoelectric effect induces a macroscopic electric field.

Inserting these quantities in (6) we find the boundary velocity v_B and the modification of the Seebeck coefficient by the slip length,

$$\delta\alpha_b = \delta\alpha\frac{1+b/\lambda}{1+2b/a}. \tag{12}$$

The overall behavior is similar to (8), yet with a linear correction term b/λ that is by a factor 2 smaller. This difference is readily traced back to the fact that thermophoresis is quadratic in the surface potential, whereas the electric field $\mathbf{E}_\infty$ couples linearly to ψ_0.

V. DISCUSSION.

According to Eqs. (8) and (12), the Soret and thermoelectric effects of charged colloids show a similar dependence on a finite slip length b. For small values of b we find an enhancement factor proporotional to the ratio of slip and Debye lengths b/λ. If b is comparable to the particle size, this linear law saturates at a constant value $\sim a/\lambda$.

A recent experimental study [7] reported the thermophoretic mobility D_T of charged polystyrene beads to depend on the particle size. The data show a linear variation with both particle radius and Debye length, $D_T \propto a\lambda$, in the range 2nm $< \lambda <$ 13nm and 10nm $< a <$ 550nm. These observed dependencies are well accounted for by Eq. (8) with slip boundary conditions, $\lambda \ll a \ll b$, but differ essentially from the no-slip result $D_T^{(0)} \propto \lambda^2$. Yet note that a fit of these data with Eq. (8) would require a slip length of hundreds of nanometers. Such large values are hardly realistic in view of available data [27]. Moreover, a large slip length implies high surface tension, i.e., low solubility of the particles. Thus we feel that at present there is no satisfactory explanation for the data of [7].

As a more promising system for the observation of slip-enhanced thermophoresis, one could think of thermally driven flow through a pore or in a microchannel. This situation is accounted for by our results when putting in the above formulae $a \to \infty$. Then the enhancement factors in Eqs. (8) and (12) read $(1+2b/\lambda)$ and $(1+b/\lambda)$, respectively. A significant enhancement is expected it the slip length b exceeds the Debye length λ, which is typically of the order of one nanometer.

[1] W. Köhler, S. Wiegand (eds.): *Thermal Nonequilibrium Phenomena in Fluid Mixtures*, Springer (2001)
[2] R. Piazza, A. Parola, J. Phys. Cond. Matt. **20**, 153102 (2008)
[3] R. Piazza, A. Guarino, Phys. Rev. Lett. **88**, 208302 (2002)
[4] S. Iacopini, R. Piazza, Europhys. Lett. **63**, 247 (2003)
[5] R. Kita, S. Wiegand, J. Luettner-Strathmann, J. Chem. Phys. **121**, 3874 (2004)
[6] S.A. Putnam, D.G. Cahill., Langmuir **21**, 5317 (2005)
[7] S. Duhr, D. Braun, PNAS **103**, 19678 (2006)
[8] S. Iacopini et al., EPJ E **19**, 59 (2006)
[9] S.A. Putnam et al., Langmuir **23**, 9221 (2007)
[10] R. Kita, P. Polyakov, S. Wiegand, Macromolecules **40**, 1638 (2007)
[11] D. Vigolo, G. Brambilla, R. Piazza, Phys. Rev. E **75**, 040401 (2007)
[12] M. Braibanti et al., Phys. Rev. Lett. **100**, 108303 (2008)
[13] H. Ning et al., Langmuir **24**, 2426 (2008)
[14] S. Duhr and D. Braun, Phys. Rev. Lett. **97**, 038103 (2006).
[15] E. Ruckenstein, J. Colloid Interface Sci. **83**, 77 (1981)
[16] K.I. Morozov, JETP **88**, 944 (1999)
[17] A. Parola, R. Piazza, EPJ E **15**, 255 (2004)
[18] S.N. Rasuli, R. Golestanian, **101**, 138101 (2008)
[19] S. Fayolle, T. Bickel, A. Würger, Phys. Rev. E **77**, 041404 (2008)
[20] A. Würger, Phys. Rev. Lett. **101**, 138102 (2008)

[21] A. Würger, Phys. Rev. Lett. **98**, 138301 (2007)
[22] E. Bringuier, A. Bourdon, PRE **67**, 011404 (2003)
[23] S. Fayolle et al., Phys. Rev. Lett. **95**, 208301 (2005)
[24] J.K.G. Dhont et al., Langmuir **23**, 1674 (2007)
[25] J. L. Anderson, Ann. Rev. Fluid Mech. **21**, 61 (1989)
[26] C. Neto et al., Rev. Prog. Phys. **68**, 2859 (2005)
[27] E. Lauga, M.P. Brenner, H.A. Stone, in: J. Foss et al. (ed.), *Handbook of Experimental Fluid Dynamics*, Springer (2007)
[28] L. Joly et al., J. Chem. Phys. **125**, 204716 (2006)
[29] A. Ajdari, L. Bocquet, Phys. Rev. Lett. **96**, 186102 (2006)
[30] J. Happel, H. Brenner, *Low-Reynolds Number Hydrodynamics*, Prentice-Hall, New York (1965)
[31] L. D. Landau and E. M. Lifshitz, *Fluid Mechanics*, Elsevier Amsterdam (1987)
[32] R. Golestanian, T.L. Liverpool, A. Ajdari, New J. Phys. **9**, 126 (2007)
[33] D. Einzel, P. Panzer, M. Liu, Phys. Rev. Lett. **64**, 2269 (1990)
[34] N.O. Young et al., J. Fluid Mech. **6**, 350 (1959)
[35] P.C. Hiemenz, R. Rajagopalan, *Principles of Colloid and Surface Chemistry*, Dekker (1997)
[36] D.C. Prieve et al., J. Fluid Mech. **148**, 247 (1984)